Thermal cycles effects on interlaminar shear strength (ILSS) and impact behaviour of carbon/PEI composites

TAMER SINMAZÇELİK*
Mechanical Engineering Department, Kocaeli University, Veziroglu Campus, İzmit, Turkey; TUBITAK MCTRI, P.O. Box 21, 41470, Gebze, Turkey
E-mail: tamersc@yahoo.com

A. ARMAĞAN ARICI
Mechanical Engineering Department, Kocaeli University, Veziroglu Campus, İzmit, Turkey

Published online: 4 February 2006

In this paper, the effect of thermal cycle on the interlaminate shear strength (ILSS) and impact behaviour of unidirectional carbon fibre reinforced polyetherimide (PEI) matrix composites were studied. Samples were subjected to 100 thermal cycles (by immersing from boiling water (100°C) to ice water (0°C). The effects of thermal cycles were characterized by short beam shear and instrumented impact testers. Also Fractographic investigations were done using a scanning electron microscope (SEM). It is observed that the plastic deformations at the fibre/matrix and interlaminar interface as well as residual stresses lower the ILSS and flexural modulus of the material proportional with the number of thermal cycles. Up to the first 20 thermal cycles the material shows a brittle fracture with lower fracture energy, but after the 20th thermal cycles it is possible to observe that the material fractures with higher fracture energy at longer fracture time. A remarkable difference in the fracture morphology between the thermal cycled and un-treated materials has been observed. It is found that thermal cycles strictly affect the fracture morphology.

1. Introduction

Unidirectional carbon fibre reinforced polyetherimide (PEI) matrix composites are being used increasingly in aerospace and aeronautic industries. These materials are widely used in aircraft bodies. Aircrafts are exposed to atmospheric environments during service life. Composite materials are subjected to attacks of the environment and must be used under moisture at different conditions. Thus the environmental effect of moisture and/or water absorption at different temperatures on carbon fibre reinforced polymeric composites is of significant interest because the mechanical and physical properties are greatly dependent on it. The water absorption, not surprisingly, results in drop of interlaminar shear strength due to degradation of PEI matrix and fibre/matrix interface [1].

When a component is subjected to cyclic temperature variation during operation, the component is described as being exposed to "thermal cycling". Thermal cycling is another serious problem for the material of aircraft bodies; because during flights at higher altitudes the temperature of the aircraft body decreases below −50°C and then may rise sharply to over 100°C in a minute time. These thermal cycles repeat along the service life. Thermal cycling induces microcracking of the resin matrix and degradation by means of shear loading [2]. Thermal exposure combined with mechanical loading can produce significant damage accumulation in polymer composites that can alter their mechanical and permeability properties [3–6].

All materials expand or contract during temperature changes. Thermal fatigue might be damaging for structures internally constrained, which cannot expand or contract freely as in composite materials. The composite consists of two distinct components: the matrix and the fibre, each with different mechanical properties and coefficients of thermal expansion. During thermal cycling, both matrix and fibre expand or contract,

*Author to whom all correspondence should be addressed.
0022-2461
DOI: 10.1007/s10853-005-3661-5

according to their coefficients of thermal expansion. As they are internally constrained, temperature fluctuations cause stress build-up at the interface [7]. These stresses might be relieved by one or more of the following means: (a) plastic deformation of the ductile matrix; (b) cracking or failure of the brittle fibre; (c) failure of the fibre/matrix interface [8]. Several simple models of fibre debonding were discussed by Hutchinson and Jensen [9]. Constraint of thermal expansion causes thermal stresses, which may also initiate and propagate fatigue cracks [10]. This, in turn, influences the structural integrity of the composite and can limit the life of a composite material. Various methods have been used to measure and quantify the effects of thermal cycling. Variations of longitudinal coefficients of thermal expansion with a number of cycles were monitored in [11]. The effect of thermal cycling was related to the amount of accumulated plastic strains in [12]. Two different damage mechanisms in Kevlar 49-epoxy composites were studied in [13]. By Bechel et al., Laminates were submerged in liquid nitrogen (LN2) and returned to room temperature 400 times. Ply-by-ply micro-crack density (transverse cracks), micro-crack span, laminate modulus, and laminate strength were measured as a function of thermal cycles in [3].

To understand the fibre-matrix interaction during temperature fluctuation extensive finite element analyses of the model have been performed the results of which are presented else in [14–16]. An axisymmetric model, shown in Fig. 1, with two rectangles representing the fibre and the matrix was analyzed. If the rectangles in Fig. 1 had not been bonded to each other during temperature fluctuations, they would expand or contract freely in the radial and axial directions according to their coefficients of thermal expansion, as shown in the upper part of Fig. 1. On the other hand if two rectangles had been bonded together, the resin would experience tensile stresses in the axial direction during the cooling portion of the thermal cycle because the matrix would contract much more than the fibre, as displayed in Fig. 1a. During the heating phase, the resin expands more than the fibre, which results in compressive axial stresses in the resin, as shown in Fig. 1b.

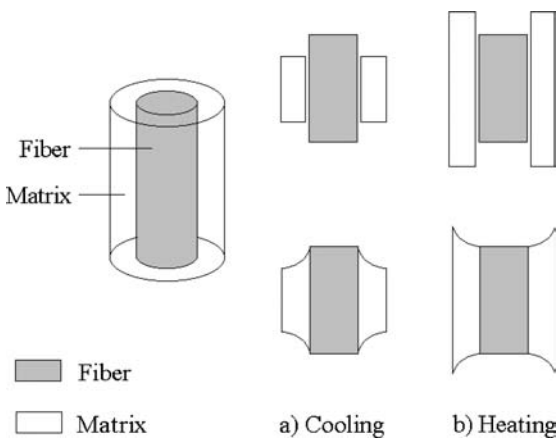

Figure 1 A cylinder of fiber embedded in cylinder of matrix.

These stress and deformation patterns allow for qualitative explanation of the mechanics of plastic deformations during thermal cycling. It should be noted that during cooling the tensile radial stress would have a tendency to tear the matrix apart from the fibre at the free surface.

Instrumented impact test is one of the important mechanical characterization techniques, which gives detailed information about the impact properties of the materials. It is possible to monitor both elastic and plastic energy absorption as a function of time or displacement. This is very important for composite materials, because it is possible to observe the energy absorption of delaminations during the impact. On the other hand short beam shear test is one of the important tests for the investigation of interlaminar shear strength (ILSS) of composites.

The objective of this study is investigating the thermal cycle and water absorption effects on unidirectional carbon fibre reinforced polyetherimide (PEI) composites. It is aimed to determine the decrease of interlaminar shear strength (ILSS) and impact strength as a function of thermal cycle. Furthermore it is aimed to determine the relationship between ILSS and impact strength. Scanning electron microscope (SEM) investigations were done to understand the fracture morphologies after water absorption and thermal cycles.

2. Experimental

Unidirectional carbon fibre reinforced polyetherimide (PEI) composites were kindly supplied by Ten Cate Advanced Composites (Nijverdal/Netherlands) in the form of hot pressed plaques. PAN based carbon fibre was manufactured by Amoco used in composite plaques (T300 12K 309 NT type). The fibre volume content is 60%. Plaques were manufactured from 14 ply with a per ply thickness of 0.14 mm and the arial weight per ply is 222 g/m^2. The commercial code of the laminate is CD5150. Mechanical properties of the composite laminate are given in Table I.

Both impact and short beam shear test samples were dried in an oven at 24°C for 24 h and then balanced before the thermal cycling tests. Thermal cycling was performed in a self-designed apparatus composed of two separate tanks consisting of a boiling water tank an ice-water tank. The temperature was kept at 100°C for the boiling water tank and 0°C for the ice-water tank. Both impact and shear test samples were placed into the sample holder and immersed into the first chamber. After waiting for 1 min in boiling water, the sample holder was raised from the first tank and immersed quickly into the second tank, which was full of ice-water. After waiting for 1 min in ice-water, samples were immersed back into the boiling water. This operation takes two minutes in total and corresponds to one thermal cycle. After the 5th, 10th, 20th, 40th, 60th, 80th and 100th thermal cycles 10 impact and 10 shear test samples were collected from the sample holder. After carefully balancing, samples were dried in an oven at 24°C for 24 h. In order to examine the variation of laminates

TABLE I Mechanical properties of composite laminate

	−55°C	23°C	80°C	80°C[a]	Units	Method
Tensile strength (0°)	1583	1890	1728	1605	MPa	ASTM D3039
Tensile modulus (0°)	131	128	127	127	GPa	ASTMD3039
Tensile strength (90°)				26	MPa	ASTMD3039
Compressive strength (0°)	936	876	814	689	MPa	ASTMD3410
Compression modulus (0°)	120	119	120	123	GPa	ASTMD3410
In plane shear strength	121	104	94	89	MPa	ASTMD3518
In plane shear modulus	4395	3208	2744	2558	MPa	ASTMD3518
Flexure strength		1289	1072	1118	MPa	ASTMD790
Flexural modulus		99	100	97	GPa	ASTMD790

[a]Pre-conditioned at 70°C/85% RH (1000 hr).

physical properties after cyclic thermal loads, short beam shear test and instrumented impact tests were carried out.

In order to obtain the interfacial strength of the carbon/PEI composites short beam shear tests were performed using an Instron 4411 tester. Composite specimens with dimension of 6×2×12 (mm) are used. The ratio of span to thickness was set to be 6, and the nose diameters of the loading cylinder and the supporting fixtures were 6.3 and 3.2 mm, respectively, as recommended by ASTM D2344-84. The crosshead speed was set to be 1 mm/min. Ten samples were tested for each parameter and the mean value of these samples was given as result.

Impact tests were performed on a instrumented Ceast pendulum type tester (Resil 25). Impact test samples were prepared according to ISO 180 standards. Un-notched samples were used with dimensions of 10×2×65 mm. Preliminary experiments were performed in order to find the appropriate falling angle, which was chosen to be 50° in order to remove the inertial oscillations in the contact load between striker and sample. At a falling angle of 50° the strike range of the izod hammer was 1.08 kN. The hammer length and mass were 0.327 m and 1.254 kg, respectively. The sampling time was 8 μsec. The impact velocity was 1.51 m/s, and the maximum available energy was 0.54 J. F_{max} is the maximum force that is obtained during the impact test. E_{max} is the total fracture energy of the material. The force-time curves can be divided into two regions: the first region is the crack initiation region and the second region is the crack propagation region. The areas under each region give the energy for these processes, which are defined as the energy for crack initiation (E_i) and the energy for crack propagation (E_p). The spikes in the first region of the F-t curve are due to inertial oscillations of the sample. Instrumented impact tests were performed with ten samples for each parameters and mean value of these samples was given as result.

Fractured surfaces of the impact test samples were examined by scanning electron microscopy, (SEM), using a JOEL JSM-6335F field emission scanning microscope.

3. Results and discussion

After 100 thermal cycles no remarkable weight change in the composite materials is observed. The results of interlaminar shear strength (ILSS) are illustrated in Fig. 2. As seen in Fig. 2 there was a remarkable decrease in ILSS even after the first 5 thermal cycles. Interlaminar shear strength was calculated for un-treated material as 85.28 MPa and 59.05 MPa for the the 5 times thermal cycled sample. Percentage decrease in ILSS after the first 5 thermal cycles corresponds to % 69.3. ILSS of the materials continued to decrease with increasing of the thermal cycles, but this amount was not as remarkable as the decrease obtained in the first 5 cycles.

During the thermal cycles the composite material was subjected to thermal stresses. After waiting in hot water at 100°C for 1 min both carbon fibres and matrix expanded. Then, materials were quickly immersed into the ice-water tank. The temperature difference was approximately 100°C. As a result of the difference in the coefficient of linear thermal expansion between the fibre and matrix, shear stresses will occur and as a result of this stresses plastic deformations and micro cracks at the fibre/matrix and interlaminar interface is expected. Also thermal gradient occurs in the composite material during the heating and cooling phases, which results in high residual stresses in plies. Like a fatigue experiment, deformations increase with the number of cycles.

During the investigations of interlaminar shear strength of composites by the short-beam method we also measured the flexural modulus of the samples. It is observed

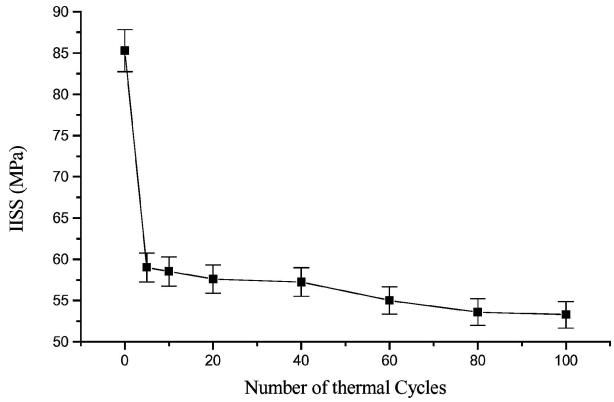

Figure 2 ILSS results as a function of thermal cycle number.

that the flexural modulus decreased as a function of the thermal cycle number (Fig. 3).

The plastic deformations at the fibre/matrix and interlaminar interface (i.e debonding, delaminations) and residual stresses lower the ILSS and flexural modulus of the material even after the first 5 thermal cycles.

Instrumented impact test results are illustrated in Figs. 4–7. As seen in Fig. 4, F_{max} values were slightly increased up to the first 20 thermal cycles. After 20 thermal cycles, F_{max} values are to decrease. The smallest F_{max} value is obtained at the 100th cycle.

Fig. 5 illustrates the total fracture energies of the materials. As seen in Fig. 5 the total fracture energy was decreased in the first 20 thermal cycles. At the 20th cycle E_{max} shows a minimum. E_{max} increased as a function of the thermal cycle number after 20 cycles. It is possible to explain the decrease in E_{max} at the first 20 thermal cycles by residual stresses, which are induced by thermal cycles. This residual stresses between the fibre/matrix and interlaminar interface were not high enough to form plastic deformations, micro crack formations or interlaminar delaminations but stretched the material. Stretched material was more inclined to initiate cracks.

Fig. 6 gives detailed information about the crack formation and propagation and their relationship to thermal

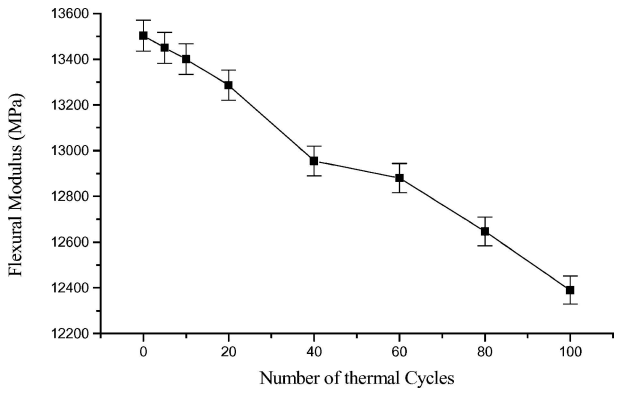

Figure 3 Flexural modulus results as a function of thermal cycle number.

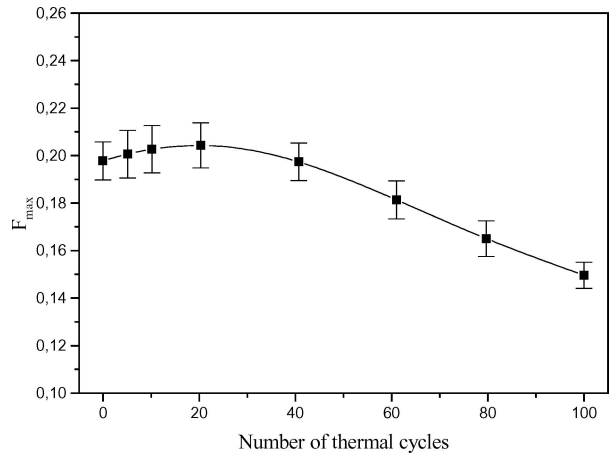

Figure 4 Impact test results (F_{max}) as a function of thermal cycle.

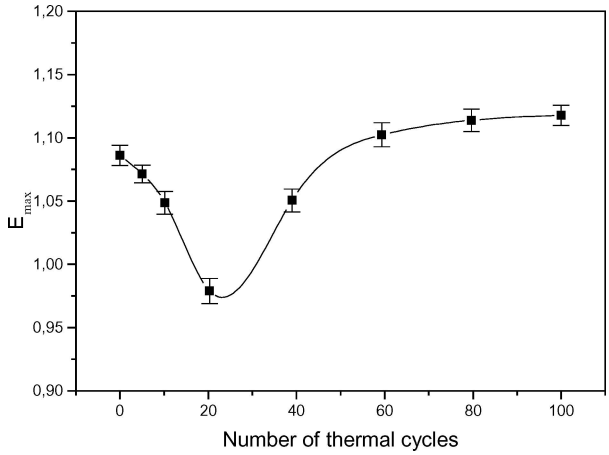

Figure 5 Impact test results (Fracture energy) as a function of thermal cycle.

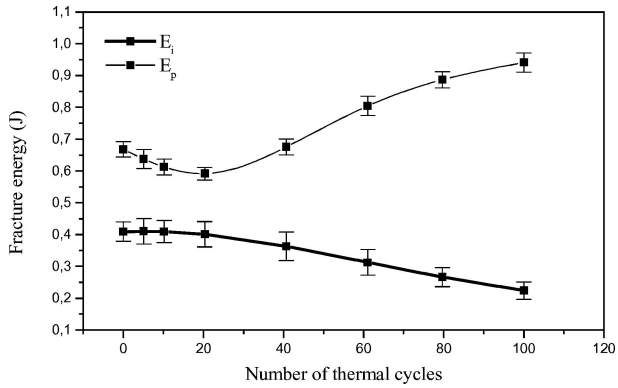

Figure 6 Impact test results (Crack initiations and propagation energies) as a function of thermal cycle.

cycles. It was clearly seen that crack initiation energy (E_i) was decreasing with increasing number of thermal cycles. On the other hand crack propagation energy was obtained to decrease slightly up to 20 thermal cycles. At the first 20 cycles it is possible to say that residual stresses help cracks to propagate easily, which result in lower the crack propagation energy. Because there were no debonded or delaminated regions and the material still behaves a brittle nature. It is understood that the thermal cycle number of 20 is a critical point in our study. At the 20th thermal cycle residual thermal stresses result in shear stresses, which were high enough to form crazes, micro cracks, delaminated or debonded regions. After 20 thermal cycles the weakening of the interface as a result of deformations permits a rise of the fracture energy, the debonding, dewetting, pull out of fibres and sliding of the fibre in the matrix blocks allowing large energy consumption until the rupture of the fibres. It was observed that there was an increase in E_p. As illustrated in Fig. 5, the total impact energy E_{max}, (sum of E_i and E_p) increases with the number of thermal cycles. We get the similar results with ref. [17].

Fig. 7 illustrates the force-time (F-t) curves of instrumented impact tests. Each force-time curves illustrates

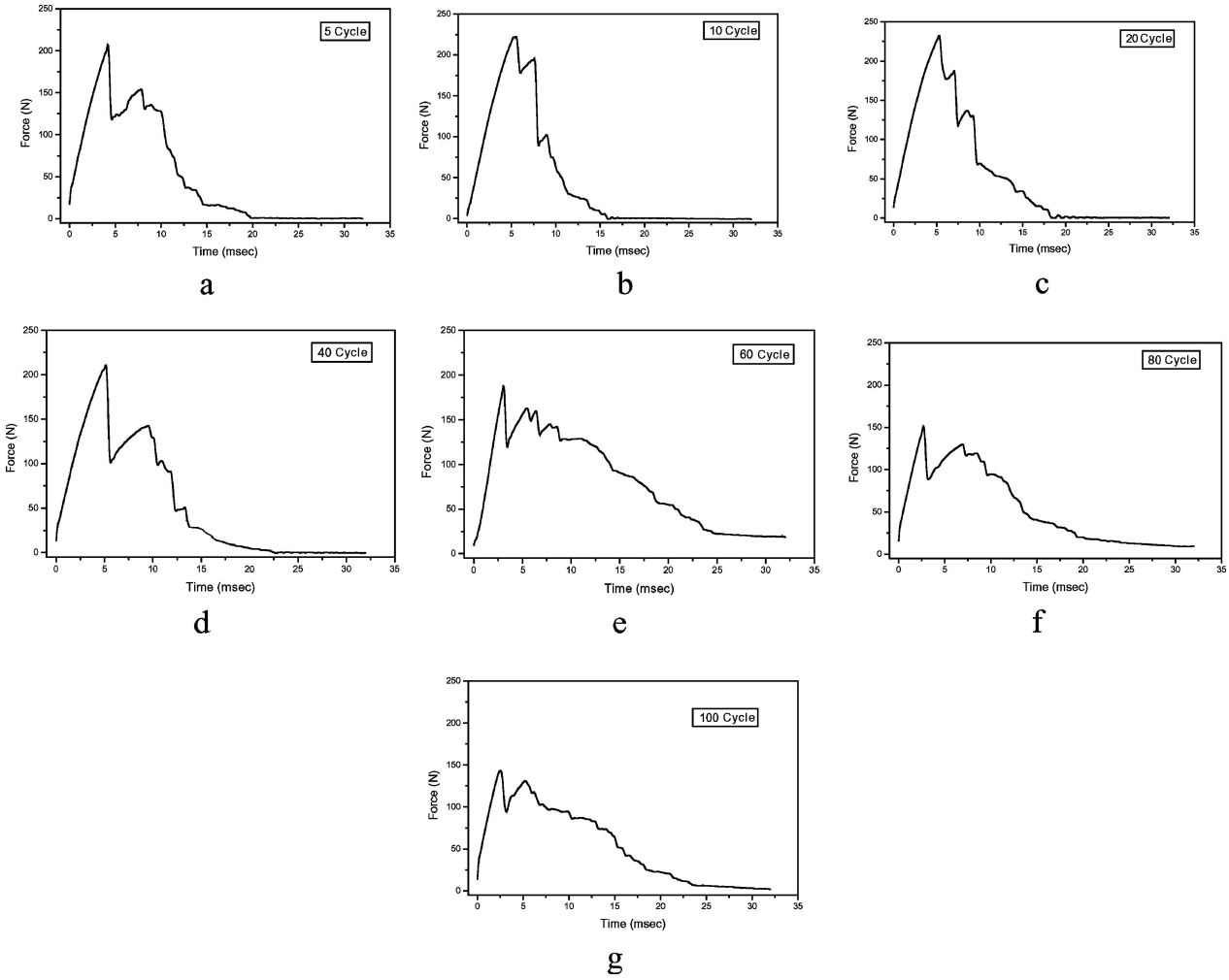

Figure 7 Force-time (F-t) curves of instrumented impact tests. There is a remarkable difference between the fracture patterns of thermal cycled material.

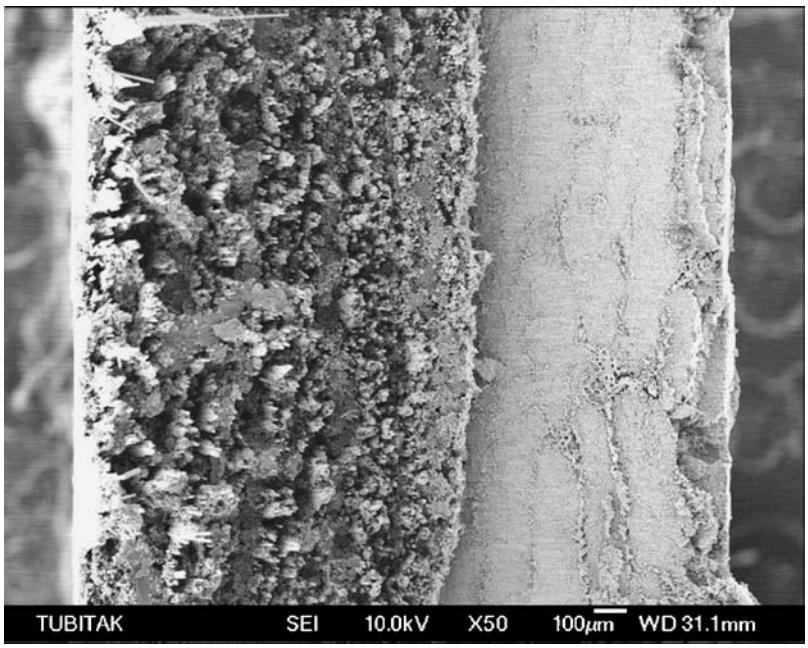

Figure 8 Fractured cross section of original sample.

single test group data, which represents the best characteristics of their group. There was a remarkable difference between the fracture patterns of thermal cycled material. Up to the first 20 thermal cycles the material shows a brittle fracture with higher F_{max} and lower fracture energy, but after 20th thermal cycles it is possible to observe that the material fractured with higher fracture energy and longer fracture time.

Fractographic investigations were done by SEM studies. Fig. 8 illustrates the cross sections of fractured untreated or original materials. It is possible to observe the neutral axis, tensile zone and compression zones clearly. Neutral axis divides the fractured cross sections into two parts. The tensile zone is placed on the left hand side while the compression zone is placed on the right hand side. Un-treated material with a strong interface tends to show brittle-like planar fracture surfaces the brittle fracture morphology is clearly observed in Fig. 8.

Fig. 9 illustrates the fractured cross sections of a 100 times thermal cycled samples. There was a remarkable morphological difference as compared to untreated material (Fig. 8). There was not a evident neutral axis formation

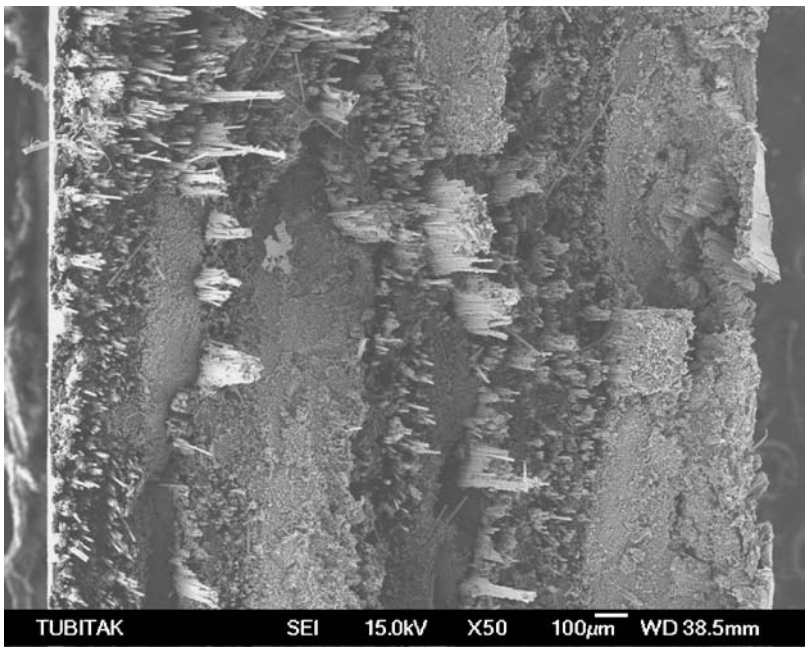

Figure 9 Fractured cross section of 100 times thermal cycled sample.

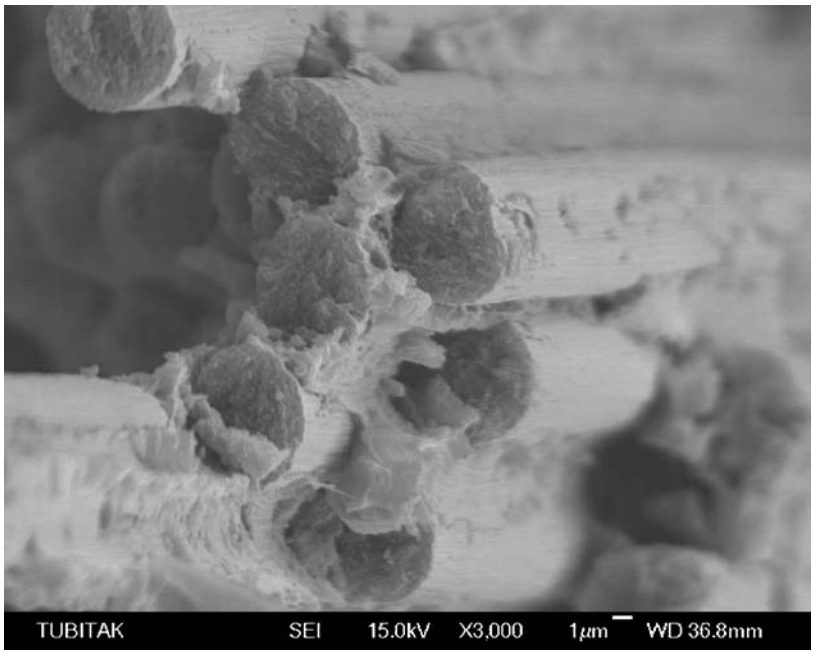

Figure 10 Boundry layer of tensile zone of fractured untreated material.

as observed in Fig. 9. As a result of thermal cycles delaminations between the plies (or laminates) occur in the material. Each laminate was fractured individually with mixture of tensile-compression zones placed around the cross sections. Weak-interface materials exhibited brush-like failures with protruding fibres. It is also possible to observe longer debonded, pulled out fibre bundles at the cross sections, which indicate the poor interfacial bonding and weakened zones between the fibre/matrix and inter-laminar interfaces.

Fig. 10 shows the boundary layer of the fractured untreated material surface of the sample at the tensile zone. The fracture of a fibre bundle in the composite specimen with PEI matrix was observed. The fibres seem to be bonded very strongly to the matrix. The high interfacial strength between the fibre and matrix leads eventually to extensive transverse fibre fracture on the back face of impact rather than pulling-out of fibres, matrix cracking, etc. Fibres fractured in a brittle manner without any indication of yield or flow. As a result of

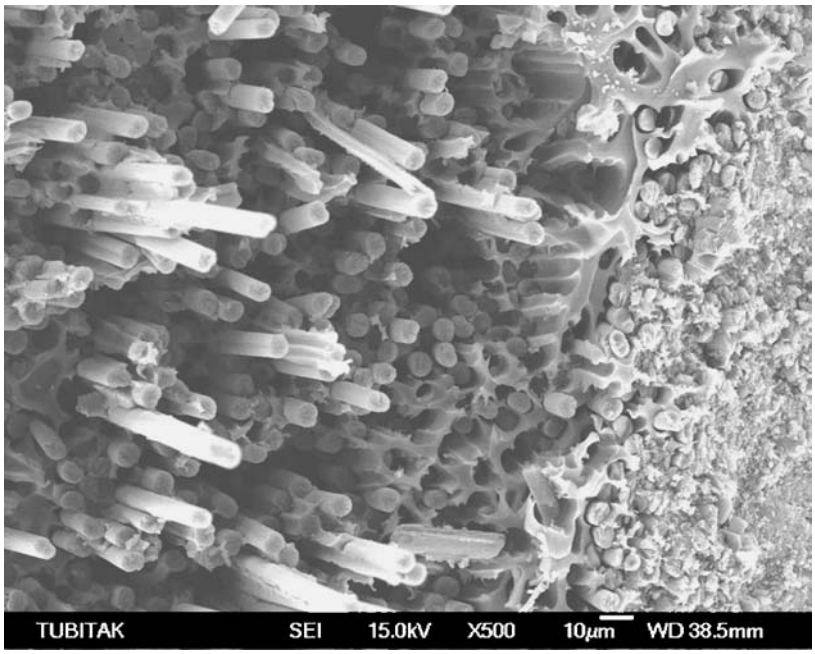

Figure 11 Tensile zone of fractured cross sections of 100 times thermal cycled sample.

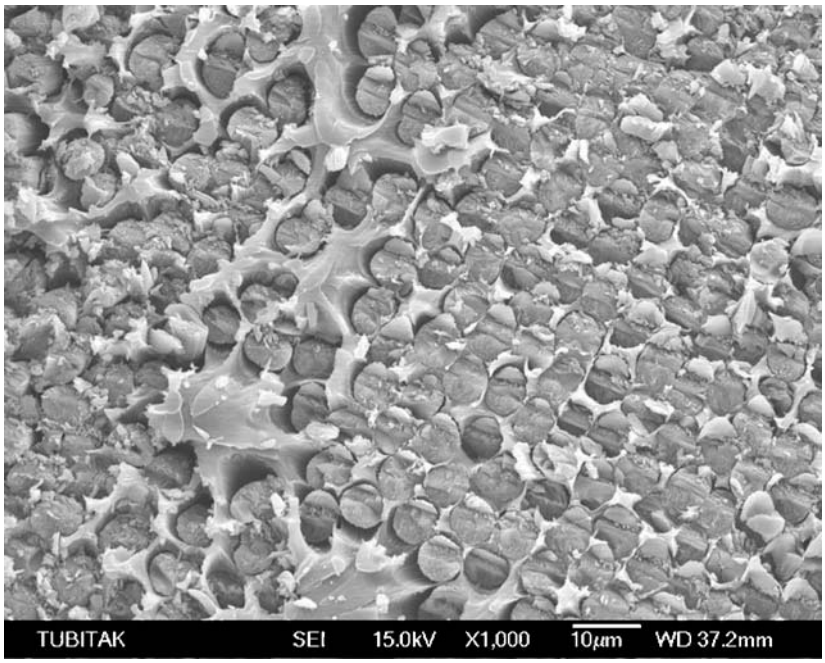

Figure 12 Compression zone of fractured cross sections of untreated material.

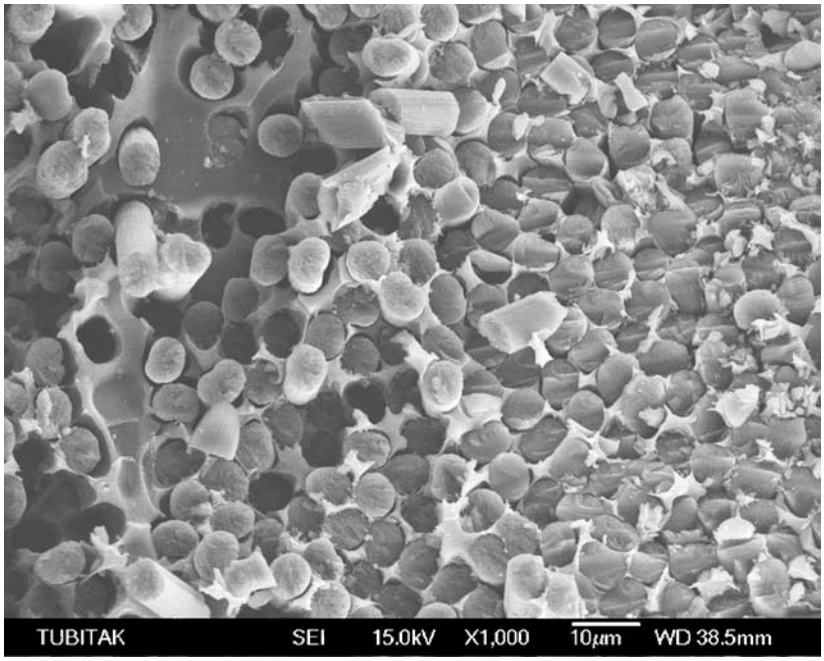

Figure 13 Compression zone of fractured cross sections of 100 times thermal cycled sample.

strong fibre-matrix interfacial bond strength, the pull-out lengths show a very short stub of carbon fibre.

As a result of thermal cycle, there was a remarkable deformation in the fibre/matrix interface. It is possible to see many pulled long fibres, which indicate poor adhesion between the fibre/matrix interfaces as shown in Fig. 11. The length of pulled-out fibre is quite longer than fractured untreated material.

There was a brittle fracture wrinkled pattern on the fracture surface of all fibres in the compression zone of untreated material (Fig. 12). In addition to shear fractured fibres, small fibre fragments as a result of microbuckling and the fracture of resin can be observed in Fig. 12. Fracture of the polyetherimide matrix was formed in irregular patterns including the matrix fragments of 0.5–5 μm sizes. The extensive fragmentation of the matrix can be attributed to compression and shear fracture from the impact loading and can be contrasted with the matrix fracture occurring under quasi-static loading conditions.

Fig. 13 illustrates the compression zone of thermal cycled material. It should be remembered that as a result of thermal cycles, there were a remarkable stresses and elasto-plastic deformations at the fibre/matrix interface. Weakening at the interface resulted in insufficient support of fibres by the matrix. Increased debonded fibre length caused more available fibres to be fractured by microbuckling deformations. It is possible to see in Fig. 13 that there were fractured short fibres and many pulled out fibres on the cross sections.

4. Conclusion

The residual stresses at the fibre/matrix and interlaminar interface as a result of thermal cycles lowered the ILSS and flexural modulus. The percentage decrease in ILSS after the first 5 thermal cycles corresponds to % 69.3. ILSS of the materials decreased with increasing thermal cycle number, but this increase was not as remarkable as in the first 5 cycles. Remarkable differences between the fracture patterns of thermal cycled materials were observed. Up to the first 20 thermal cycles material showed a brittle fracture with higher impact force and lower fracture energy. After 20 thermal cycles it is possible to observe that the material fractured with higher fracture energy and longer fracture time.

Thermal cycling results in weak fibre/matrix and interlaminar interfacial strength. This causes remarkable difference in fracture morphology. As the fractured cross sections were investigated it was observed that material changes its fracture morphology from brittle to though manner.

References

1. M. HUSSAIN and K. NIIHARA, *Mater. Sci. Engng. A* **272** (1999) 264.
2. K.-B. SHIN, C.-G. KIM, C.-S. HONG and H.-H. LEE, *Composites: Part B* **31** (2000) 223.
3. V. T. BECHELA, M. B. FREDINA, S. L. DONALDSONA, R. Y. KIMB and J. D. CAMPINGB, *Composites: Part A* **34** (2003) 663.
4. K. AHBORN and S. KNAAK, *Cryogenics* **28** (1988) 273.
5. S. L. DONALDSON and R. Y. KIM, in Proceedings of the 47th SAMPE International Symposium, Long Beach, CA (1991) pp. 1248.
6. A. T. NETTLES and E. S. BISS, in "Low Temperature Mechanical Testing of Carbon-Fiber/Epoxy Resin Composite Materials". NASA Technical Memorandum, NASA Center for Aerospace Information, (1996) TM-1996-3663.
7. K. BIERNACKI, W. SZYSZKOWSKI and S. YANNACOPOULOS, *Composites: Part A* **30** (1999) 1027.

8. S. YANNACOPOULOS, J. R. HILDERBRANDT and S. O. KASAP, in "Thermal Fatigue of Fiber Reinforced Composites, Advanced Composites in Emerging Technologies, in edited by S.A. Paipetis, T.P. Philippidis, (1991) p. 253.
9. J. W. HUTCHINSON and H. M. JENSEN, *Mechani. Mater.* **9** (1990) 139.
10. D. A. SPERA, in "What is Thermal Fatigue in Thermal Fatigue of Materials and Components", in edited by D.A. Spera, D.F. Mowbray, Philadelphia, PA:, American Society for Testing and Materials, (1975), vol. 3.
11. W. L. MORRIS, M. R. JAMES and R. V. INMAN, *J. Engng. Mat. Tech.* **111** (1989) 331.
12. R. C. WETHERHOLD and L. J. WESTFALL, *J. Mat. Sci.* **23** (1988) 713.
13. S. J. DETERESA and L. NICOLAIS, *Polym. Compo.* **9** (1988) 192.
14. W. SZYSZKOWSKI and J. A. KING, *Computers Struct.* **56** (1995) 354.
15. J. A. KING, in "Numerical Stress Studies in Composites," MSc thesis, University of Saskatchewan, Saskatoon, Canada, 1995.
16. A. ABEDIAN and W. SZYSZKOWSKI, *Composites A.* **28** (1997) 573.
17. V. BIANCHI, P. GOURSAF and E. M. CNESSIERB, *Comp. Sci. Techn.* **58** (1998) 409.

Received 16 August 2004
and accepted 25 May 2005